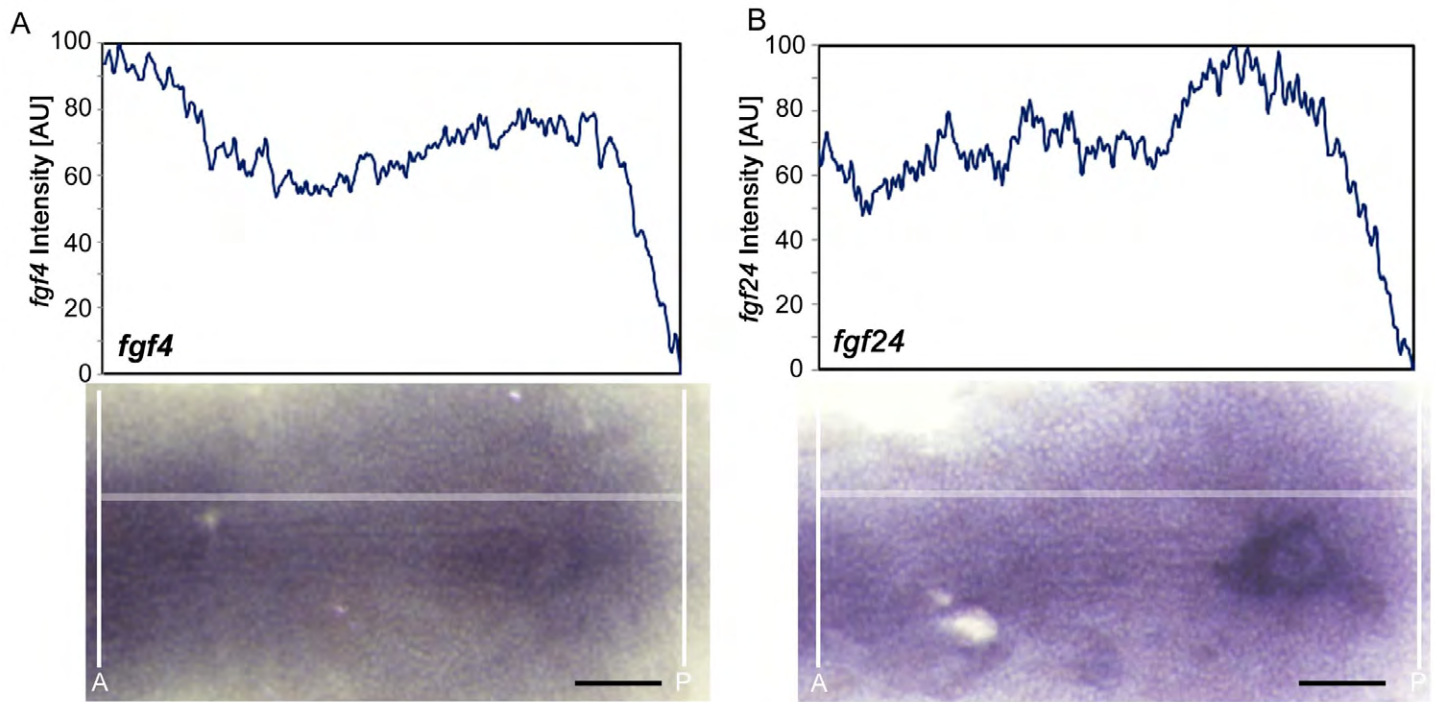
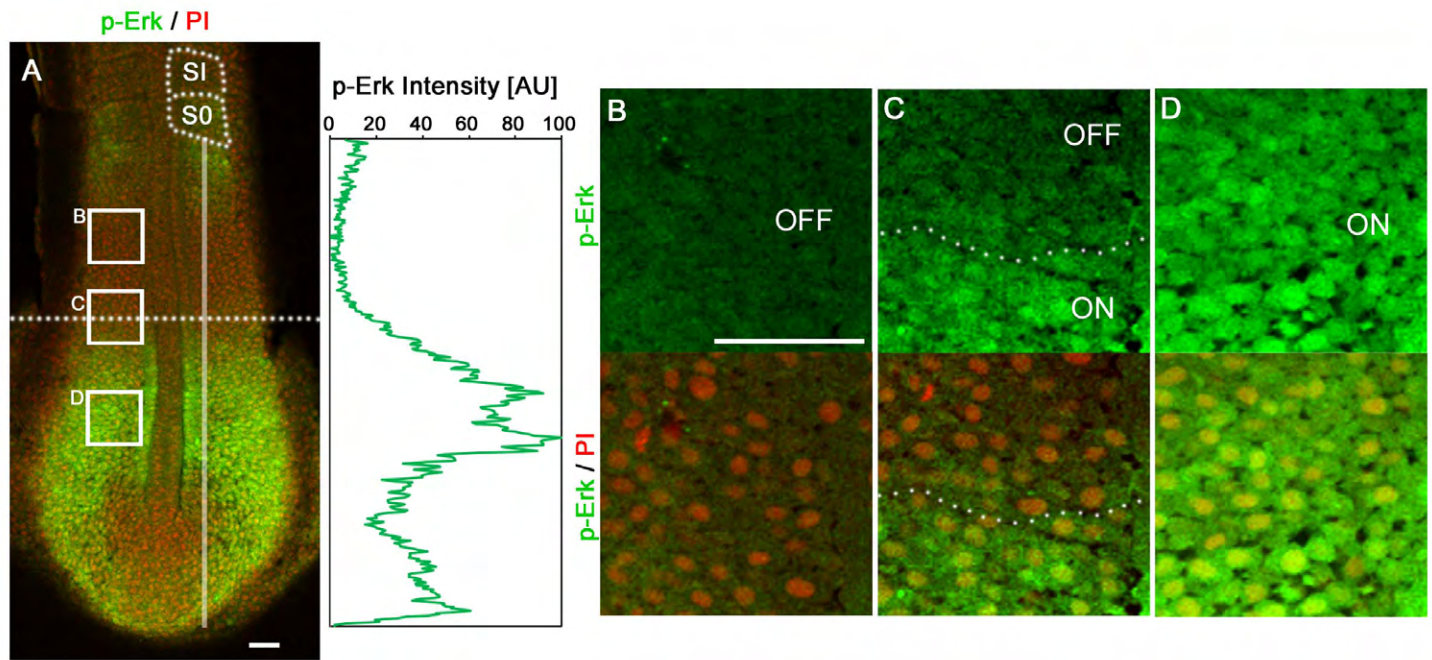


**Figure S1. *ace/ace* embryos (*fgf8a* mutants) shows segmentation defects.** (A-C) Representative images of p-Erk signals (A), *mesp-b* (B) or *uncx4.1* expression (C) in wild-type (left panel) or *ace/ace* (right panel) embryos at 10- to 12-somite stages. Although Erk activity was reduced in the small and narrow PSM of all *ace/ace* embryos (n = 10), the Erk activity boundary could be seen (A). Consistent with the change of Erk activity at mid-somitogenesis stages, *mesp-b* expression at S-I and S-II was partially fused and patchy in *ace/ace* embryos, and the angle of *mesp-b* stripes became steeper than that of wild-type (B; 70%, n = 51). In addition, expression of *uncx4.1* became abnormal in 79% *ace/ace* embryos (C; n = 29).



**Figure S2. Neither *fgf4* nor *fgf24* mRNA shows graded distribution in the PSM.** (A, B) Representative images of *fgf4* (A) or *fgf24* (B) expression. Signal intensities (upper images; AU, arbitrary unit) were measured by ImageJ software from the original pictures (lower). Dorsal view of tailbud regions in flat-mounted embryos, anterior to the left. The horizontal white lines in the lower images mark the paths along which the signal intensities shown in the upper panel were recorded. Scale bar: 100  $\mu$ m.



**Figure S3. p-Erk distribution in the PSM.** (A) Left: flat-mounted wild-type embryo at the 6-somite stage immunostained with p-Erk antibody (green). Nuclei are stained with PI (red). Right: p-Erk signal intensity was measured along the white line shown in the left image. (B-D) PSM cells viewed at a higher magnification, p-Erk signals in the nuclei are a sign of Erk activation. In the anterior PSM, nuclear p-Erk signals were not detected (B), whereas nuclear p-Erk signals were detected in all the cells in the posterior PSM (D). A boundary of nuclear p-Erk signals could be seen at the middle of the PSM (white dotted line in panel C). Scale bar: 40  $\mu$ m.

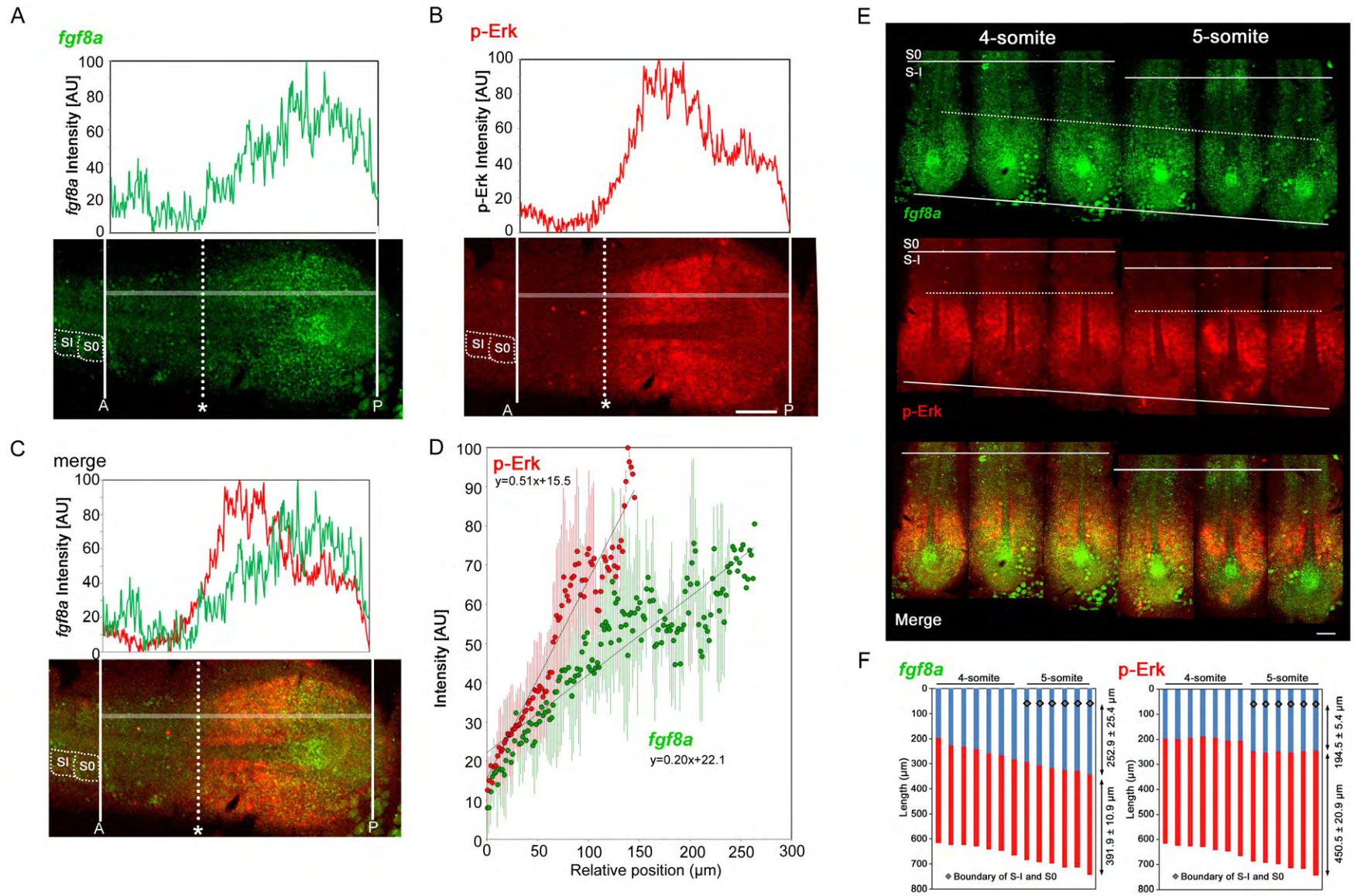
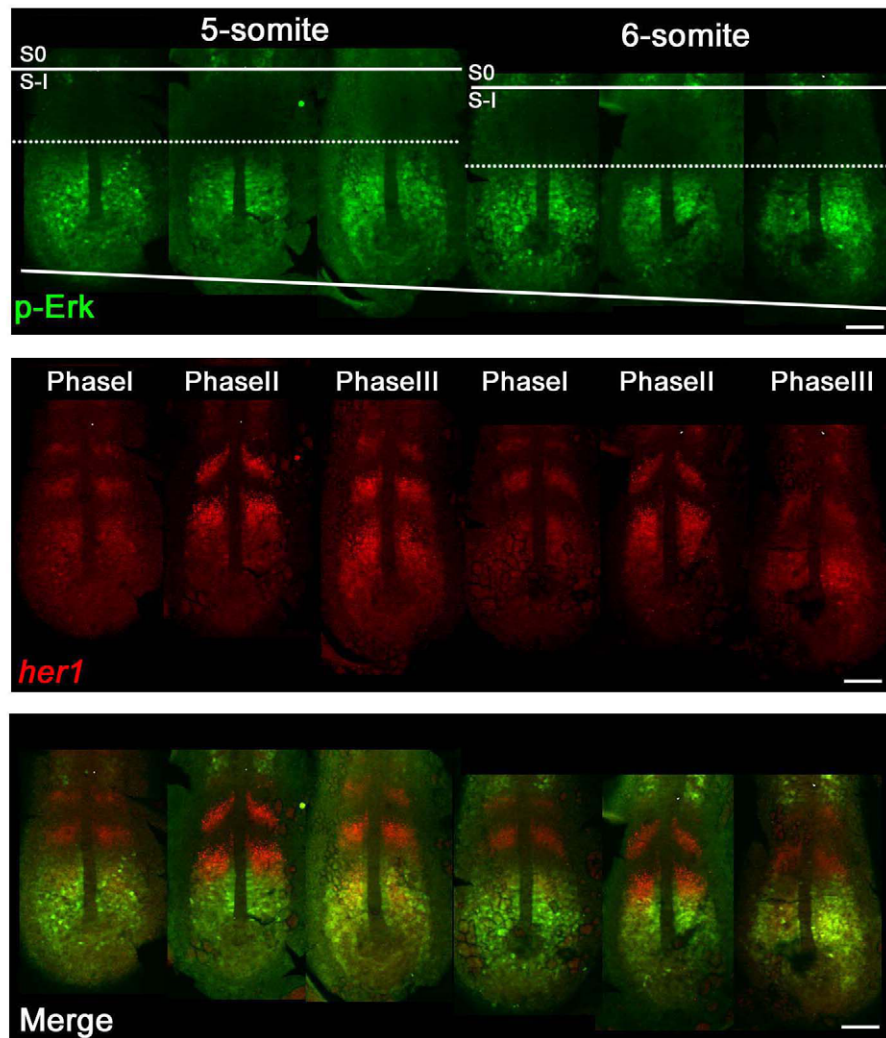


**Figure S4. Double staining of *fgf8a* and p-Erk in the same embryo.** (A) *fgf8a* expression. (B) p-Erk distribution. (C) Merged image of *fgf8a* (green) and p-Erk (red). Signal intensities (upper images; AU, arbitrary unit) were measured by ImageJ software from the original pictures (lower panels). Anterior and posterior ends of the PSM are marked by white lines. Scale bar: 100 μm. The position of the anterior extremity (dotted lines) was estimated by comparison of signal intensity (upper panel) and visual observation (lower panel). Dorsal view of tailbud region in the flat-mounted embryo, anterior to the left. The horizontal white lines in the lower images mark the paths along which the signal intensities shown in the upper panel were recorded. (D) Comparison of slopes between *fgf8a* expression and p-Erk distribution. Approximation formulae of *fgf8a* and p-Erk were calculated from average values of signal intensities, respectively (n = 7). Dots indicate averages and green/red bars indicate standard deviations. (E) Representative images of *fgf8a* expression (green) and p-Erk distribution (red) in double stained embryos at the 4- to 5-somite stages. Dorsal view of tailbud regions, anterior to the top. Scale bar: 100 μm. (F) Quantitative data of *fgf8a* expression (left) or p-Erk distribution (right) in double stained embryos (n = 13). Statistical significance of variation ( $2P < 0.05$ ) could be seen in *fgf8a* expression region (C.V. = 0.028) versus *fgf8a* non-expression region (C.V. = 0.100) and in the OFF region (C.V. = 0.028) versus the ON region of Erk activity (C.V. = 0.046).



Stage	Phase	n	OFF region ( $\mu\text{m}$ )	ON region ( $\mu\text{m}$ )
5-somite	I	4	201.3 $\pm$ 2.9	393.5 $\pm$ 6.5
	II	5	197.8 $\pm$ 3.0	419.4 $\pm$ 4.7
	III	4	202.3 $\pm$ 3.6	442.0 $\pm$ 15.0
6-somite	I	3	199.7 $\pm$ 4.2	399.0 $\pm$ 5.0
	II	4	195.8 $\pm$ 1.5	418.5 $\pm$ 6.5
	III	3	195.7 $\pm$ 0.6	443.0 $\pm$ 6.1

**Figure S5. Posterior shift of p-Erk signal coincides temporally with the transition from phase III to I of cyclic *her1* expression.** p-Erk (green) and *her1* (red) were stained in the same embryos. Embryos are displayed in order of phase propagation of *her1* oscillation (from phase I to III). Scale bar: 100  $\mu\text{m}$ . Length of p-Erk ON and OFF regions was measured and listed in the bottom table.

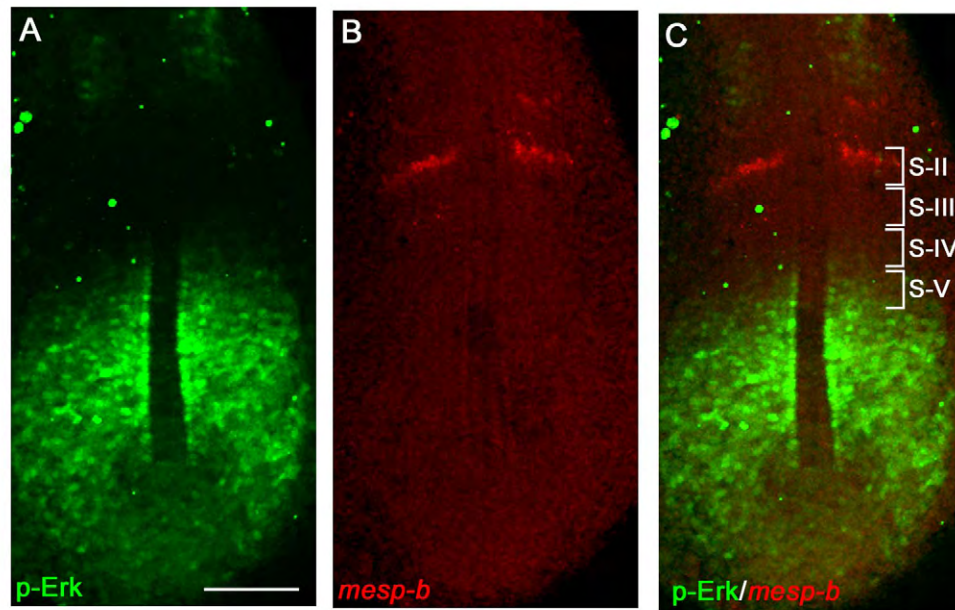


**Figure S6. Spatial distribution of p-Erk and *mesp-b* mRNA in the PSM.** Double staining of p-Erk (A, green) and *mesp-b* (B, red). Scale bar: 100  $\mu$ m. The anterior limit of Erk activity is located about three somite lengths posterior to B-2.

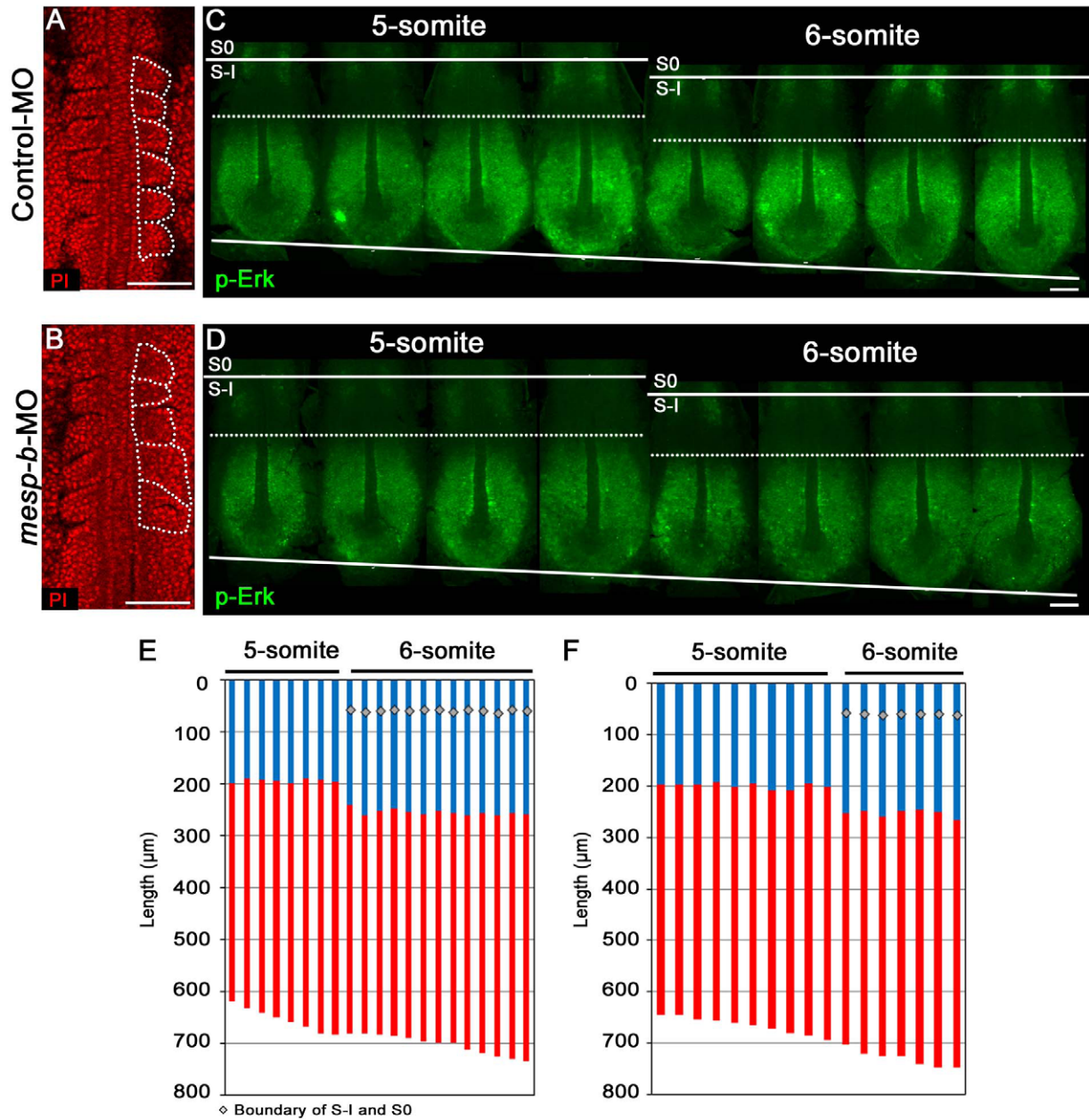


**Figure S7. Knockdown of *mesp-b* does not affect the stepwise pattern of p-Erk.** (A, B) Somite morphology in control-MO-injected (A) or *mesp-b*-MO-injected (B) embryos. Nuclei are stained by PI (red). Somites are outlined by dotted lines. Scale bar: 100  $\mu$ m. (C, D) p-Erk signals in control (C) or *mesp-b* (D) morphants at the 5- to 6-somite stages. (E, F) Quantitative data for p-Erk signals in control (E, n = 21) or *mesp-b* (F, n = 17) morphants. Even when *mesp-b* was knocked down, the stepwise movement of p-Erk occurred normally.

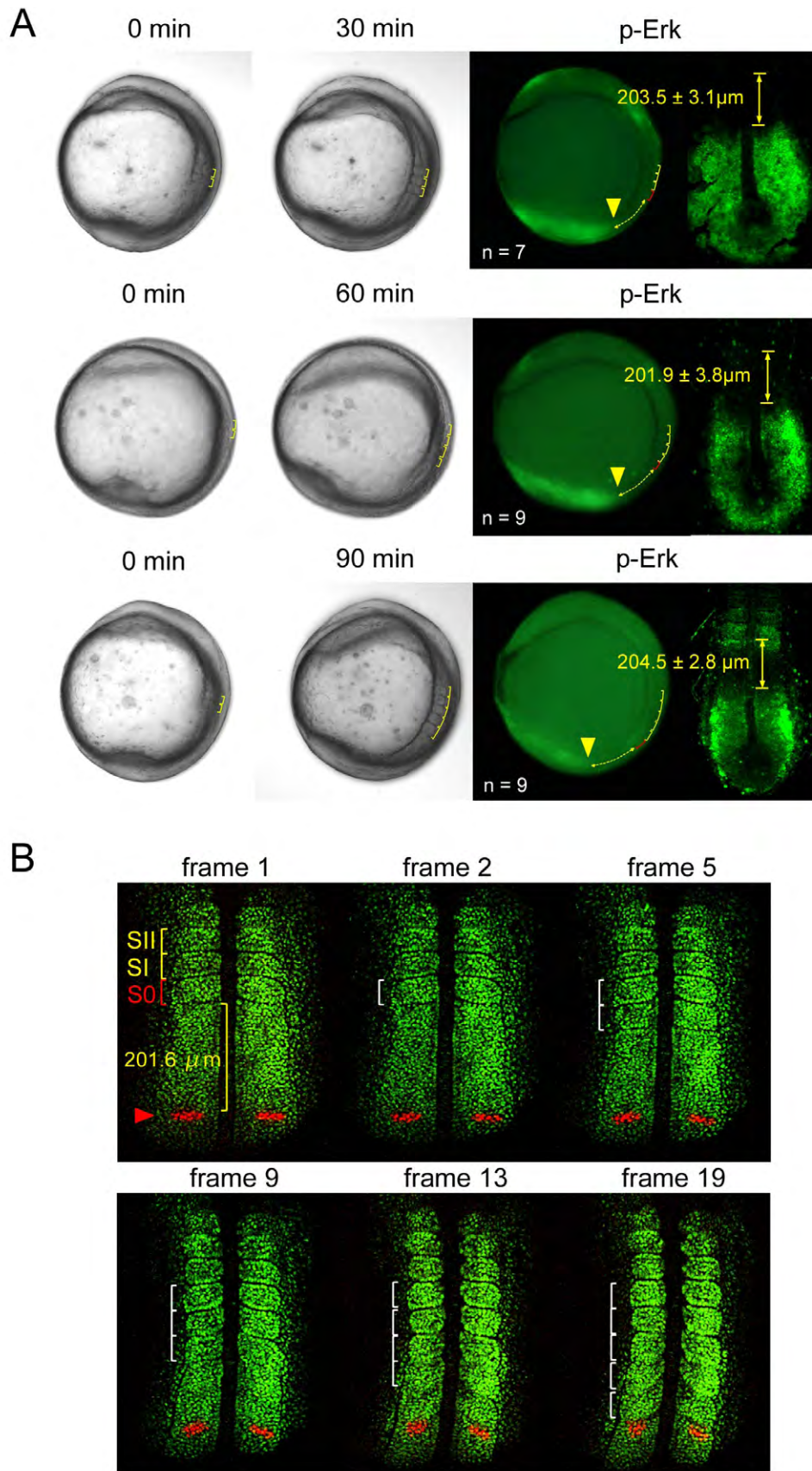


**Figure S8. The anterior limit of Erk activity represents the future somite boundary at B-5.** (A) Time-lapse imaging followed by p-Erk staining. Each embryo was immediately fixed and stained for p-Erk after somite formation was observed for 30, 60 or 90 min by time-lapse. Lateral view, anterior to the top. To measure the length of the p-Erk OFF region, the embryo was flat-mounted (right panel). Mean  $\pm$  s.d. of the OFF region length is shown. (B) Specific fluorescent labeling and time-lapse imaging. Photo-conversion of KikGR revealed that the position at about 200  $\mu\text{m}$  away from B-1 (red arrowhead) represents the future somite boundary at B-5. White brackets mark newly formed somites during time-lapse imaging. Images are frames of Movie 1.

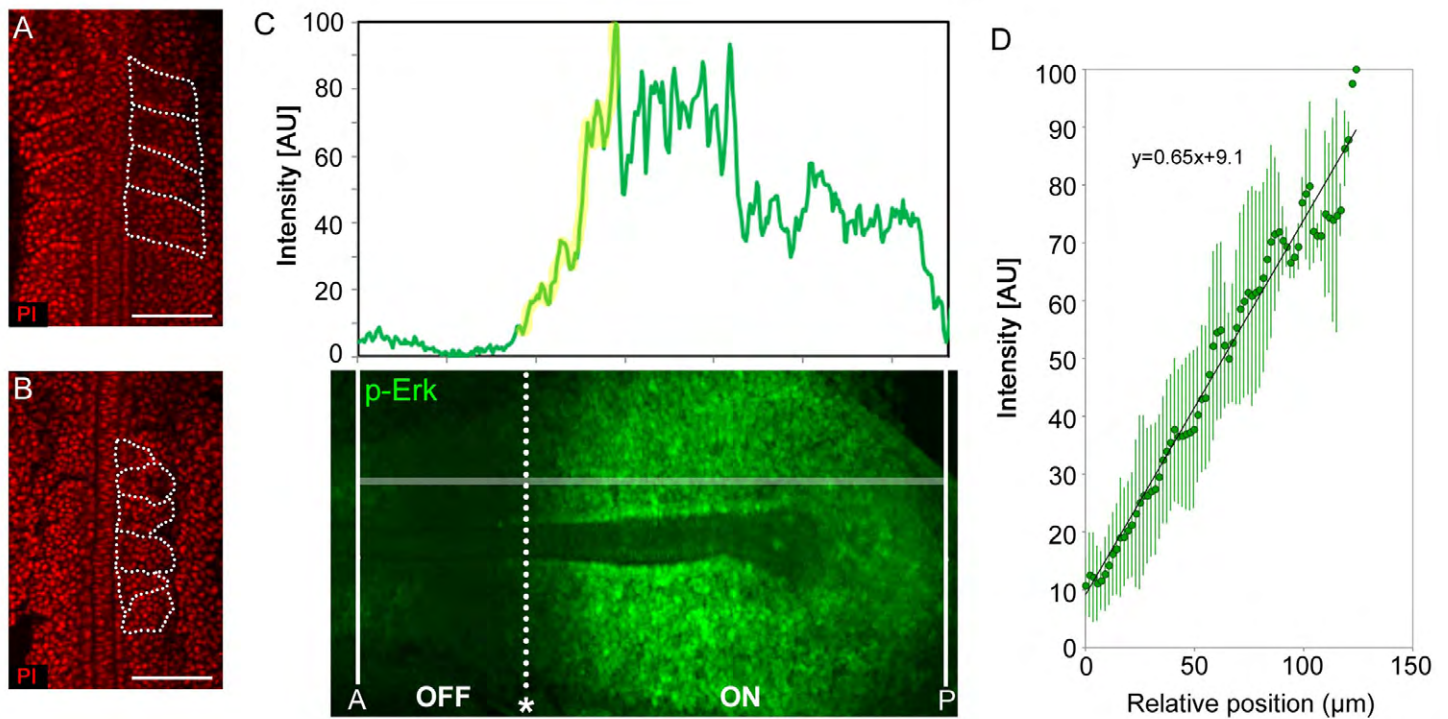


**Figure S9. Spatial distribution of p-Erk in *her1* and *her7* double-knockdown embryos.** (A, B) Somite morphology in wild-type embryos (A) or embryos co-injected with *her1*-MO and *her7*-MO (B). Nuclei are stained by PI (red). Somites are outlined by dotted lines. Scale bar: 100  $\mu$ m. Double knockdown of *her1* and *her7* disrupted the proper repetitive structures of somites. (C) Representative images of p-Erk distribution (green) showing the bimodal pattern in double-knockdown embryos of *her1* and *her7*. Signal intensity (upper image; AU, arbitrary units) was measured from the original picture (lower). Dorsal view of tailbud regions in flat-mounted embryos, anterior to the left. (D) Intensity plot of the upward slope region of the gradient represented by the yellow line in (C). Mean  $\pm$  s.d. of intensity ( $n = 7$ ) is shown. The equation describing the slope obtained from these *her1* and *her7* double-knockdown embryos is almost the same as that of wild-type (Figure 1C), suggesting that the somite segmentation clock does not affect the steepness of the p-Erk gradient.

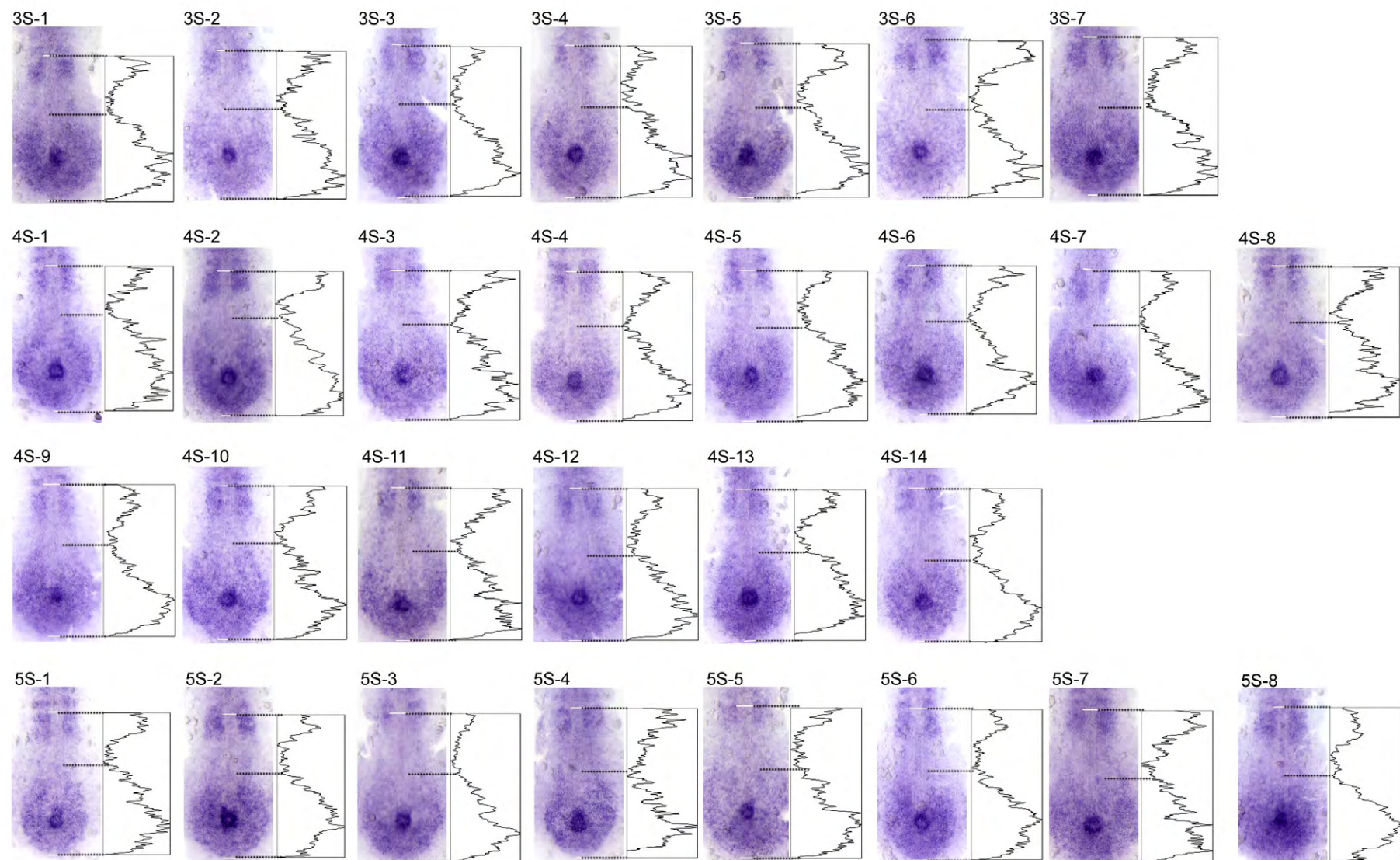


**Figure S10. Expression of *fgf8a* in wildtype embryos (n = 29).**

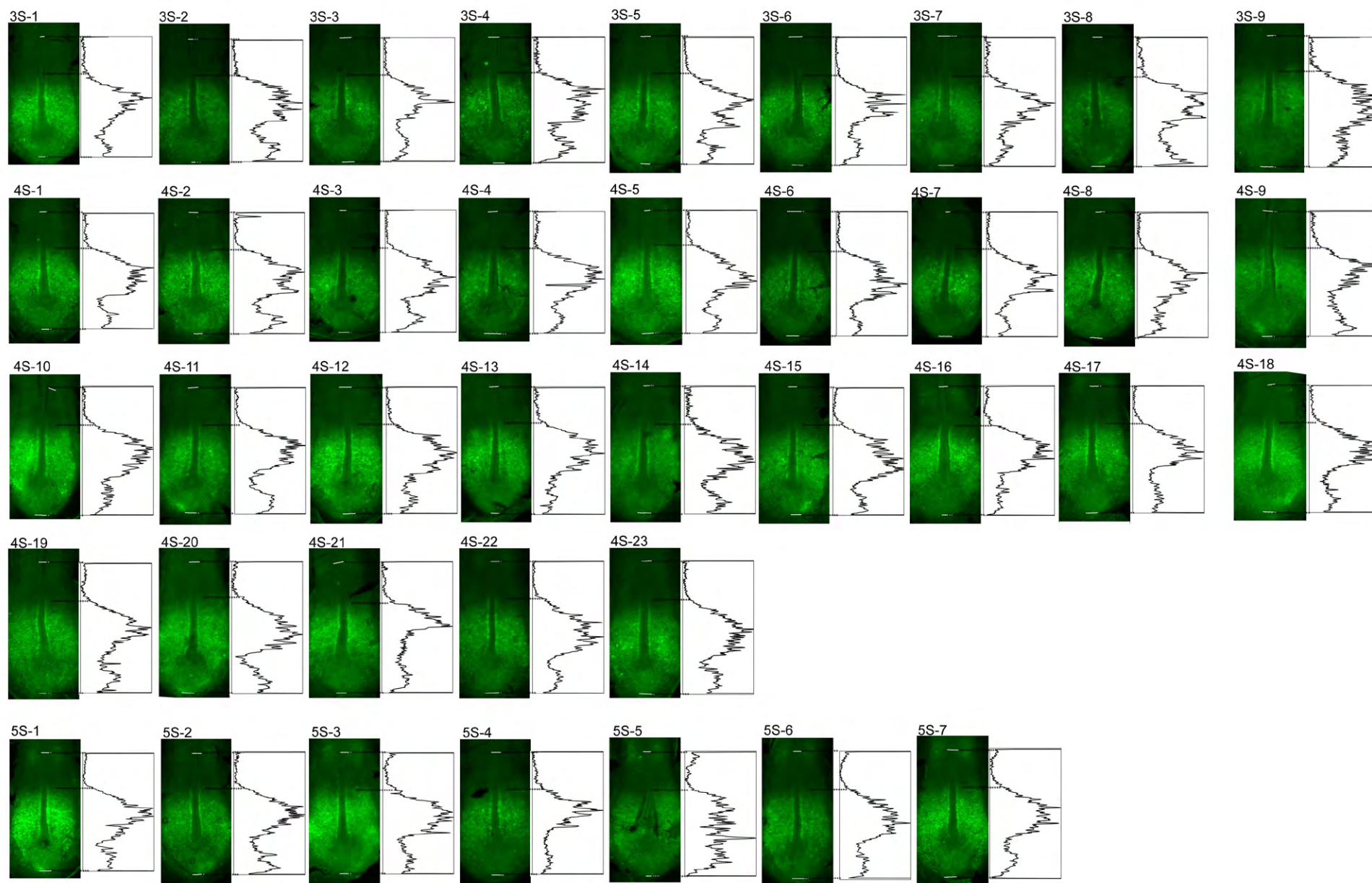


**Figure S11. Distribution of p-Erk signals in wildtype embryos (n = 39).**

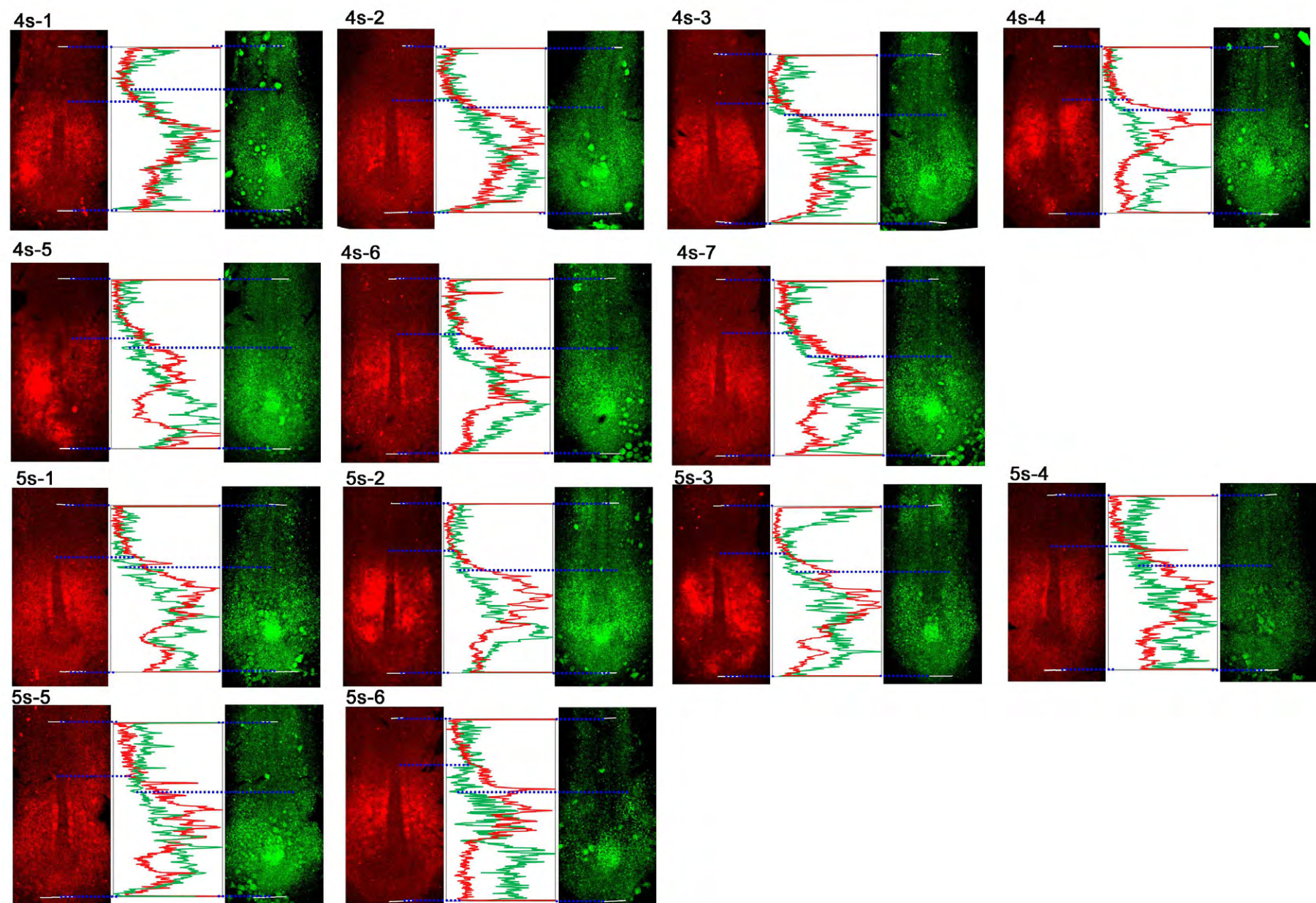


Figure S12. Expression of *fgf8a* (green) and distribution of p-Erk signals (red) in double stained embryos (n = 13).

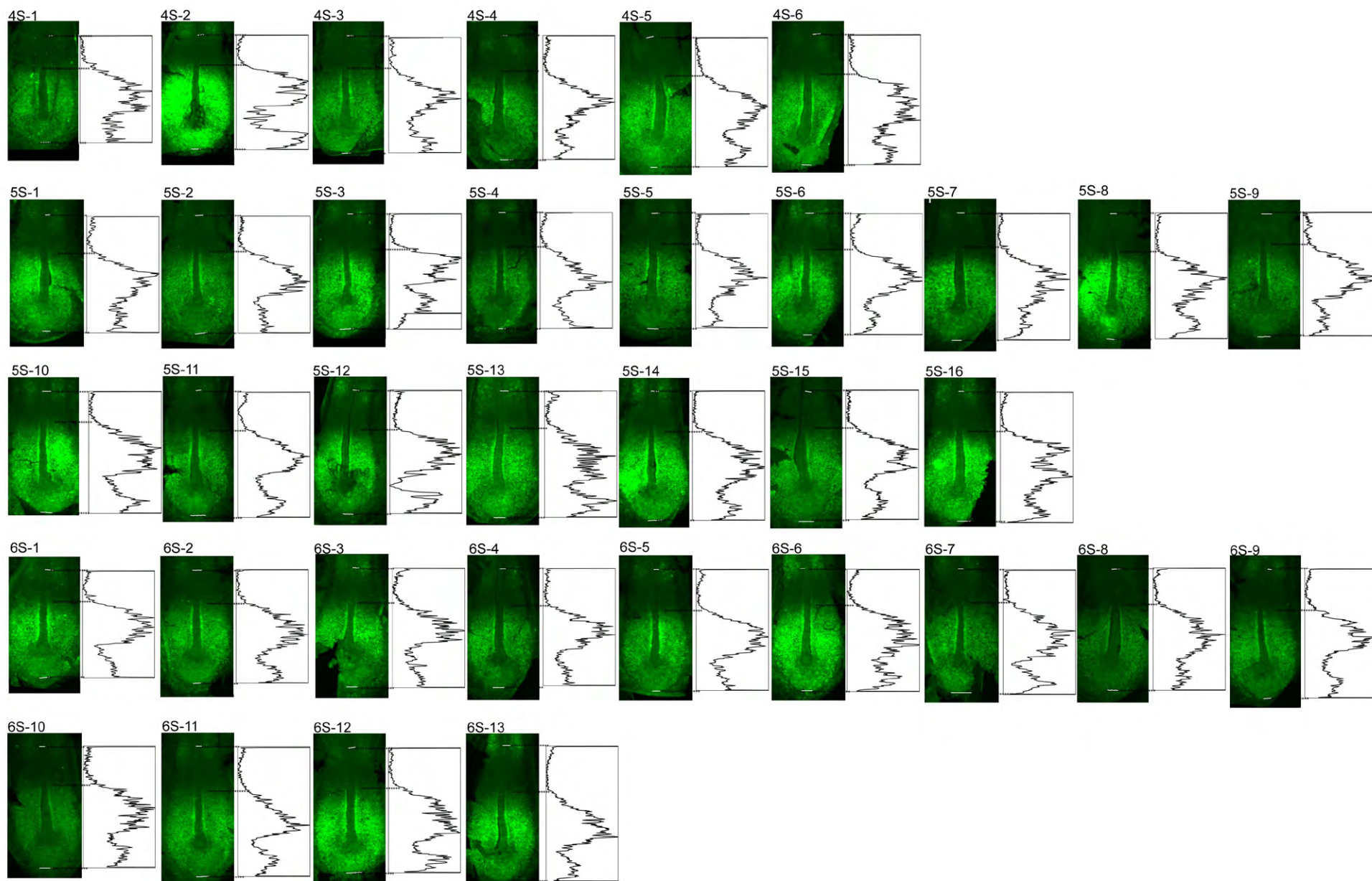
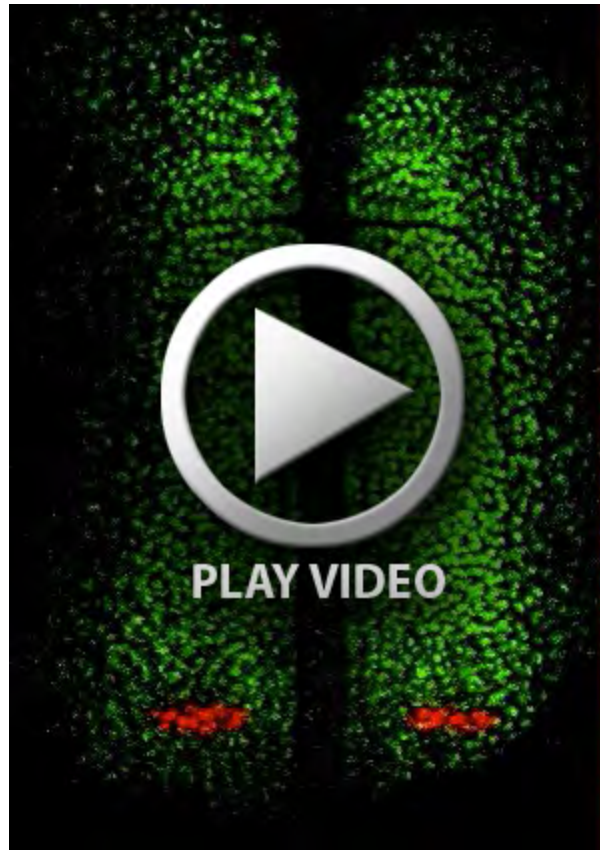


Figure S13. Distribution of p-Erk signals in *her1* and *her7* double knockdown embryos (n = 35).



**Movie 1. Time-lapse imaging of the presumptive p-Erk boundary.** This movie shows the dorsal view of a *Tg[her1:KikGR]* embryo (shown in Fig. S8B). Movements of photo-converted cells (red) located around the Erk activity boundary were traced in 5 rounds of segmentation.